

Supplementary Information

All-silicon low-loss THz temporal differentiator based on whispering gallery mode resonator waveguide platform

Yunjie Rui^{1,5}, Shuyu Zhou^{1,5}, Xuecou Tu^{1,2,*}, Xu Yan¹, Bingnan Yan¹, Chen Zhang¹,
Ziyao Ye¹, Huilin Zhang¹, Jingya Xie⁴, Qing-Yuan Zhao^{1,3}, La-Bao Zhang^{1,2}, Xiao-Qing
Jia^{1,2}, Huabing Wang^{1,3}, Jian Chen^{1,3}, Lin Kang^{1,2} and Peiheng Wu^{1,2}

¹Research Institute of Superconductor Electronics (RISE), School of Electronic Science
and Engineering, Nanjing University, Nanjing, Jiangsu 210023, China

²Hefei National Laboratory, Hefei 230088, China

³Purple Mountain Laboratories, Nanjing, Jiangsu 211111, China

⁴Terahertz Technology Innovation Research Institute, Shanghai Key Lab of Modern
Optical System, University of Shanghai for Science and Technology, Shanghai, 200093,
China

⁵These authors contributed equally: Yunjie Rui and Shuyu Zhou

*Corresponding authors. Email: X.T. (tuxuecou@nju.edu.cn)

28 **Supplementary Note 1: First-order differentiator in the time domain (IFOD)**

29 In this section, we will demonstrate that a WGMR waveguide operating in the
30 critical coupling resonance can approximate a time differentiator.

31 The basic structure of the silicon WGMR waveguide used in this study involves a
32 ring coupled to a single straight waveguide. According to the coupling mode theory, the
33 transfer function of the microring resonator can be expressed as follows:

$$34 \quad T(\omega) = \frac{s_0}{s_i} = \frac{j(\omega - \omega_0) + \frac{1}{\tau_i} - \frac{1}{\tau_e}}{j(\omega - \omega_0) + \frac{1}{\tau_i} + \frac{1}{\tau_e}} \quad (1)$$

35 where ω_0 is the resonance frequency, $1/\tau_i$ is the power decay rate due to intrinsic
36 losses, $1/\tau_e$ is the power coupled to the waveguide, and $1/\tau$ is the photon lifetime,
37 with $1/\tau = 1/\tau_i + 1/\tau_e$. When the frequency detuning is much smaller than the 3 dB
38 bandwidth of the resonator, the expression can be approximated as follows:

$$39 \quad T(\omega) = j\tau(\omega - \omega_0) + \frac{\frac{1}{\tau_i} - \frac{1}{\tau_e}}{\frac{1}{\tau_i} + \frac{1}{\tau_e}} \quad (2)$$

40 In particular, when the WGMR waveguide operates in the critical coupling resonance
41 ($\tau_i = \tau_e$), the following expression can be obtained:

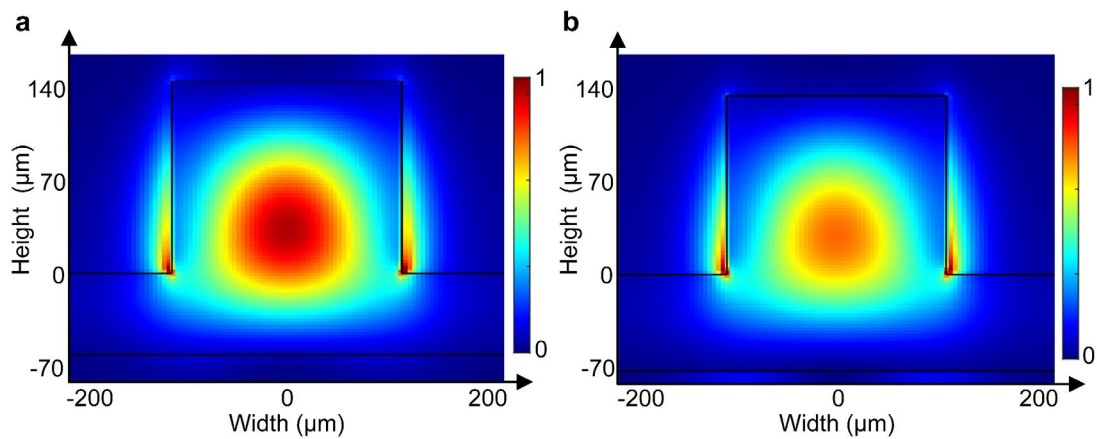
$$42 \quad T(\omega) = j\tau(\omega - \omega_0) \quad (3)$$

43 Equation (3) is essentially consistent with the transfer function of an ideal first-order
44 differentiator in the time domain.

45 **Supplementary Note 2: Waveguide dimension optimization**

46 The designed differentiator employs a ridge waveguide. The thickness of the ridge
47 waveguide substrate and the height and width of the waveguide all influence the mode
48 propagation within the waveguide. **Supplementary Figure 1a** illustrates the TE mode
49 energy distribution of the cross-section of a ridge waveguide with a substrate thickness
50 of 60 μm , waveguide height of 140 μm , and waveguide width of 210 μm at a frequency
51 of 405.45 GHz. In this dimension, the electromagnetic wave energy is well confined

52 within the dielectric waveguide, ensuring efficient transmission of the TE mode. When
53 the substrate thickness is changed to 70 μm , and the waveguide height is changed to
54 130 μm while keeping the waveguide width constant, the calculated TE mode energy
55 distribution of the ridge waveguide cross-section is shown in **Supplementary Figure**
56 **1b**. The energy at the center of the dielectric waveguide significantly weakens,
57 indicating increased transmission loss. Hence, the size of the ridge waveguide greatly
58 affects the transmission, necessitating careful design. By utilizing electromagnetic
59 simulation software, the final optimization dimensions of the ridge waveguide used in
60 the original study were determined.

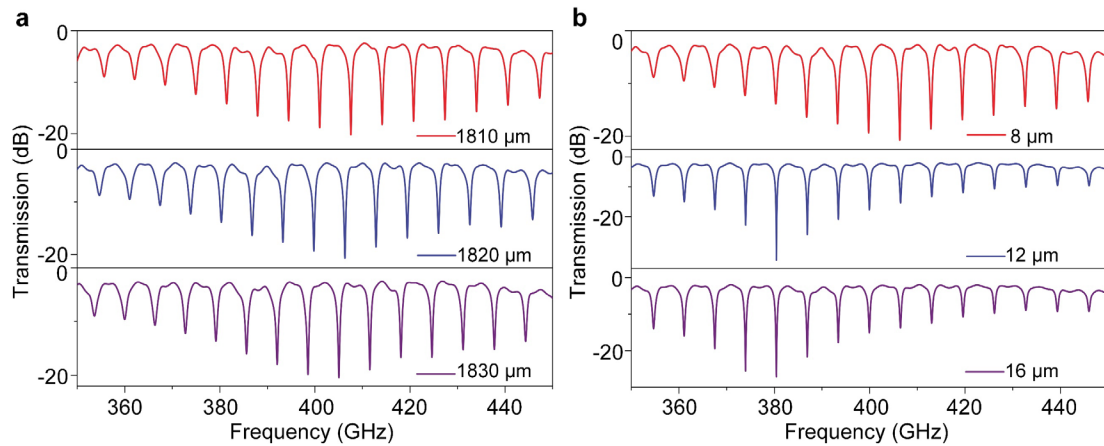


61
62 **Supplementary Figure 1:** Cross-sectional electric field distribution of the waveguide
63 at different dimensions.

64 In addition to determination of ridge waveguide dimensions, the radius of the
65 microring and the gap between the microring and the straight waveguide also influence
66 the transmission characteristics of the entire resonator. The following optimization will
67 focus on the impact of these parameters from the perspective of the WGMR
68 waveguide's transmission.

69 **Supplementary Figure 2a** shows the calculated transmission of the WGMR
70 waveguide chip obtained at different radii. It can be observed that the radius size affects
71 the position of the critical coupling point. As the radius increases, the critical coupling
72 frequency decreases. **Supplementary Figure 2b** illustrates the calculated transmission
73 of the WGMR waveguide chip at different gaps between the straight waveguide and the

74 microring. It is evident that the gap size not only affects the position of the critical
75 coupling point but also influences the depth of the resonance peak. Hence, these two
76 parameters significantly impact the resonant characteristics of the differentiator, and by
77 continuous optimization, the final dimensions of the radius and gap, as mentioned in
78 the paper, were determined.

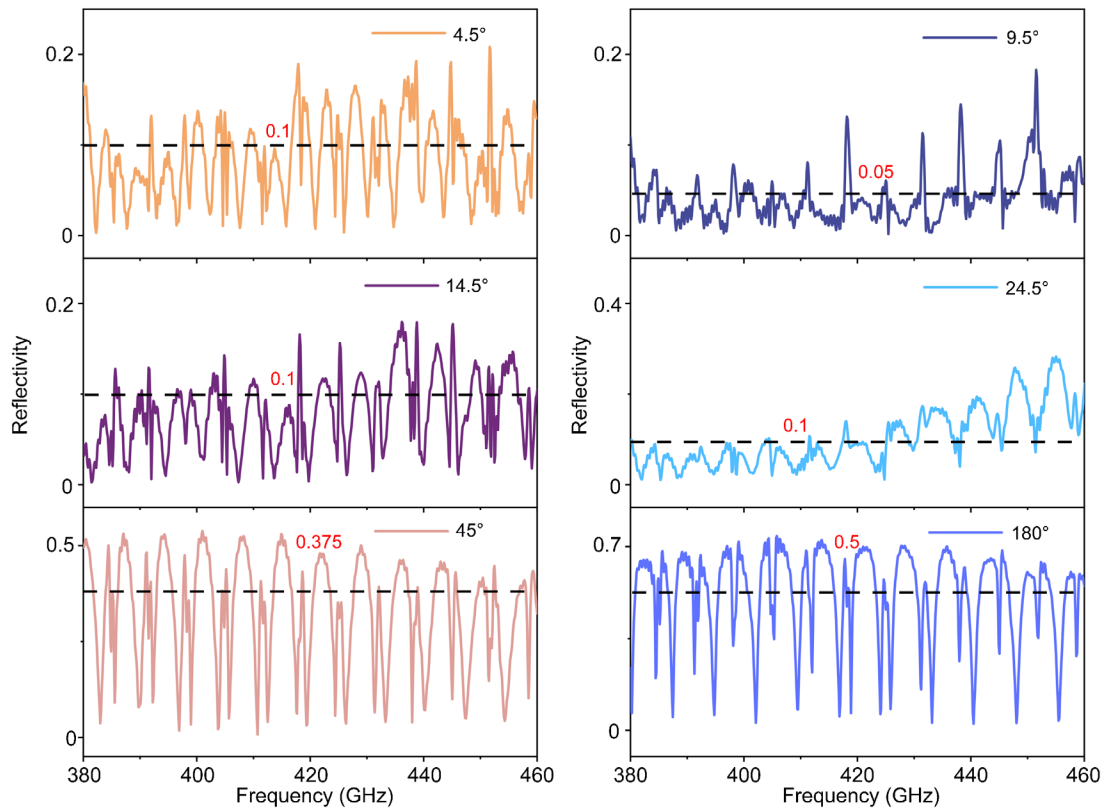


79

80 **Supplementary Figure 2:** Calculated transmission at different radii and different gaps.

81 **Supplementary Note 3: Taper angle optimization**

82 In order to mitigate the coupling loss caused by energy entering the dielectric
83 waveguide, a gradient taper structure is employed at both ends of the straight waveguide.
84 To determine the optimal taper angle of the taper, a parameter sweep is conducted on
85 the taper angle parameter (4.5° , 9.5° , 14.5° , 24.5° , 45° , 180° and so on), and the
86 reflectance of the waveguide port is calculated, as shown in **Supplementary Figure 3**.
87 The results indicate that when the taper angle is set to 9.5° , the port reflectance is below
88 0.05, significantly lower than the reflectance at other angles. In the absence of the taper,
89 the port reflectance exceeds 0.5, highlighting the necessity of incorporating the taper in
90 the WGMR waveguide chip. Furthermore, when the taper angle is set to 9.5° , the
91 calculated insertion loss is only 2.5 dB, as stated in the main text of the paper,
92 demonstrates that this angle yields high coupling efficiency and meets the design
93 requirements.



94

95 **Supplementary Figure 3:** The taper angle effect on coupling efficiency, the calculated
 96 reflectivity of the WGMR waveguide chip under different angles of the taper from 4.5°
 97 to 180°.